Research Article

Journal of Plasma Chemistry and Plasma Processing Research

New Workflow for Cryo-Electron Tomography Delivers Accurate Three-Dimensional Data Without Need of Averaging Multiple Experiments, Therefore Generating New Evidence of Mechanisms of Action

Andrea Fera, PhD*

Science Dept., Geri Anderson & Associates Inc., 12532 Westland Ct, Fulton, MD 20759

***Corresponding author**
Andrea Fera, PhD, Science Dept., Geri Anderson & Associates Inc., 12532 Westland Ct, Fulton, MD 20759.

Submitted:10 Aug 2022;**Accepted**:16 Aug 2022;**Published**:24 Aug 2022

Citation: *Andrea Fera. (2022). New Workflow for Cryo-Electron Tomography Delivers Accurate Three-Dimensional Data Without Need of Averaging Multiple Experiments, Therefore Generating New Evidence of Mechanisms of Action. J Pla Che Pla Pro Res, 3 (1): 37-42.*

Abstract

It has been recently demonstrated experimentally that, after a temperature conditioning prior exposure to the electron beam, flash-frozen biological samples (whether or not also exposed to a heavy-metal stain) resist high electron doses inside a Transmission Electron Microscope. This first proof of concept has been limited only by the resolution of the instrument used, not equipped with aberration corrector. In such conditions, published data on individual samples cannot match the Å-resolution commonly shown by cryo-electron tomograms, which data are averages over thousands of low-resolution images. Indeed, corresponding calculated structures in publications show the most probable position of each atom in the imaged proteins, obtained with a statistical Angstrom-level uncertainty. Within such instrumental limitations, the data shown here on cryo-immobilized samples are instead the first three-dimensional images documenting precisely the organization of proteins in a solution, flash-frozen in action and imaged directly, without the need to average many experiments. Therefore, these figures show only instantaneous molecular configurations. Actually, it is rather well-known that during action (i.e. during a protein-protein interaction) atoms are not necessarily in their average positions. Therefore, this new sample pre-conditioning, done at low-temperature and before exposure to the electron beam, delivers for the first-time accurate 3D measurements of protein organization in solution. This direct experimental evidence altogether, if confirmed, may constitute a basis to revisit some theoretical models describing some protein functions, e.g. for the two cases presented here, the influenza virus and tubulin, i.e. the most abundant protein in the human body.

Introduction

Historically, the invention of transmission electron microscopes (TEMs) has been motivated by the need of direct insights on structure (and functioning) of virus'and human membranes. Yet, the progress of cryo-Electron-Microscopy-Tomography (cEMT) has been hindered by the fact that in conventional cEMT protocols the electron beam is very damaging for frozen-hydrated, unstained biological samples. For this reason, conventional approach obtains high resolution (i.e. voxel sizes ≤ 1 Å3) three-dimensional (3D) data on proteins with enough signal-to-noise-ratio (S/N) only averaging data from many molecules. Which seldom are in the same atomic configuration, also because of their shallow thermal energy landscape, i.e. many configurations are equally probable at all practical temperatures (T) of interest (due to thermal vibrations). In conclusion, reaction pathways (i.e. interactions with proteins out-of-equilibrium) are presently not accessible by cEMT.

In order to address such limitations, an original approach involving a low-T pre- conditioning (TeC) of flash-frozen samples [1] has been proven able to deliver samples able to sustain, seemingly unaltered, an accelerated electron beam in vacuum for at least 1.5 hours.

Moreover, the same area can be imaged further also after storing the sample overnight. Such discovery shows a way for potentially realize, also in biology, results of the same refinement as in the material science field, where precise atomic positions can be directly measured even for dislocations in nanoparticles [2]. In fact, precise knowledge of interatomic distances (down to the pm) are necessary to develop precise force-fields and therefore models in order to comprehend interactions between molecules (and how to influence them, e.g. using small molecules).

At the current level of understanding of the mechanisms involved in the realization of such new cEMT data, it has been hypothesized that such an unexpected resistance to electron beams in vacuum may be a function of the fact that both published results [1,3] refer to rigid assembled cytoskeletal biopolymers, from human and viral

origin, bound to a metal ion. Actually, last data proved resistance to sustained irradiation weather a metal stain is bound to the protein constructs or not. In apparent contradiction to results before published [4], although the authors never explored such temperatures under vacuum. Which seems to be a key, possibly because slightly higher temperature facilitates sublimation of (free, unbound) water molecules in the conditions of the experiment [5].

Here we show TEM images obtained after TeC of very soft biological samples. Moreover, even in the limited experimental conditions in which the sample has been imaged (i.e. without aberration correctors) data on the soft model systems show recurring features, never noted before for influenza virus, which may offer new clues for modeling their behavior. On this note, we also propose some new results from the first model system published in [1] applying TeC before measuring a tomogram. Actually, taken together such images seem to suggest that it may be worth rediscussing some of current models describing assembly and functioning of such protein constructs (relative to both virus and cytoskeleton).

A few years ago, a combination of physical methods applied before imaging flash-frozen microtubules has resulted in a sample resistant to the electron beam enough to measure a full tomogram with ~110 images for a total electron dose approaching 1 million e–/nm2 [1]. Those results raised questions: (1) how much such method could be a general behavior of matter? (2) how much it depends on the stain applied to the samples before flash-freezing? (3) how softer samples will behave, with less rigidity and weaker lateral inter-molecular forces? For these reasons, recently new results have confirmed wider applicability of this method by imaging HIV capsid (CA) proteins assembled in-vitro [2]. Remarkably, it has been possible to obtain a high- resolution tomogram (with millions of electrons per nm2) both with and omitting the step of staining/fixation with a heavy metal ion [2]. The similarity between the two rigid biopolymers (from human and viral origin) prompted further investigations with more deformable materials. In this perspective, here experiments on influenza virus model systems will be shown at the limit of the resolution afforded by a TEM without aberration corrections. It is indeed interesting that, also at this limited resolution, details never shown before become apparent, which may complete current mechanistical understanding of influenza virus infection. These new results prompted as well disclosure of data obtained on microtubules imaged as [1], which also may suggest that some theoretical models accounting for microtubules formation may need to be revisited [6].

Experimental Procedures

Here we compare results obtained from tomograms of two types of samples. Both these samples have been stained with uranyl acetate (UA) before flash-freezing and then subject to the low Temperature-Conditioning (TeC) described before imaging in a TEM.

Figure 1 shows commercial influenza A virus of the Hong-Kong strain purchased by Charles River and used without further purifications. Such virus is known to become spherical and to tend to be monodisperse in dimension after many passages in chicken eggs [4] (cfr. supplementary pictures). Samples were imaged after mild centrifugation, i.e. without completely separating the allantoic fluid. After thawing in hands for ~1 minute a frozen vial from a –5ºC freezer, 10 µl was diluted to 50-100 µl with PBS solution and lightly centrifugated, if needed. An aliquot of ~6 µl supernatant was deposited on a 300 or 400 mesh formvar/C coated cupper grid (Electron Microscopy Science, EMS), and immediately mixed with a second 3 µl drop of colloidal 6 nm gold (Asurion, The Netherlands). After at least 1-2 minutes and after wicking excess of solution, a drop of 2% solution w/v of Uranyl Acetate (UA) was deposited on the grid for ~30 seconds. After wicking again, the solution excess, this drop was followed by 2 drops of Methyl-Amine Tungstate (NanoW, EMS), were the first was left in contact with grid only a few seconds before wicking the excess and depositing the second drop for ~1 minute. Grid was mounted vertical with the second drop of NanoW, wicking a last time immediately before plunge-freezing in liquid ethane, with the 'guillotine' of the laboratory where experiments were performed. Similar results were obtained more recently substituting the NanoW with a second ~ 6 µl drop of the colloidal gold solution.

All samples reported here have been imaged after applying a mixture of UA and NanoW (or only UA) before flash-freezing. This choice allowed to obtain images well-focused (at ≤ 0.5 µm defocus) and at with high-enough S/N quickly, due to time-limitations imposed by the cost of such experiments. In [2] it was demonstrated that a stain is not necessary to obtain dose- resistant frozen samples, as well the fact that data are not modified by the staining procedure at length-scales above ~0.5 nm. All experiments shown here have been possible thanks to the collaboration of local laboratories. Experiments in [1] and (Figure. 3) were performed at the NIH campus, where they were forced to stop because of a sudden, mainly unexplained, unavailability of suitable TEMs. The decisive round of experiments was privately financed by Geri-Anderson and Associates Inc. (GAA) using microscope facilities at the University of Maryland Global Campus and at the University of Virginia Charlottesville, Medical School. This last laboratory especially actively contributed to the realization of the conditions necessary for such experiments, not completely standard in their line of work.

From a first evaluation of the images, it appears that the position of the colloidal gold was not completely random. In fact, the last purification steps of Asurion involve glucose cushions [*private communications*], so that it is possible that highly electronegative Aun+ ions may have bound poly-glucosides, known to interact with receptors on hemagglutinin. Certainly, colloidal gold appeared not randomly distributed on the grid.

Flash-frozen grids were inserted, under liquid nitrogen, in a cryo-holder pre-cooled by liquid nitrogen. After mounting the holder inside a Transmission Electron Microscope (TEM) samples

were temperature-cured (TeC) as described before [1-2]. With this procedure not-bound water molecules sublimate from the sample [5-6] before exposing it to an electron beam, accelerated at 200 or at 100 keV for the experiments shown here.

This preconditioning at low temperature in vacuum seems the critical step. The time needed actually seems to scale with the time necessary for the spontaneous sublimation of frozen water (in the experimental conditions described [6]). Such time is inversely proportional to factors like degree of hydrophobicity of the sample, hydrophobic compartments, residual unbound water accumulated inside membranaceous convoluted compartments in soft samples... Many of these factors are not easily quantifiable and therefore trial-and-error was adopted. In fact, the only sample imaged after TeC until now that has not shown any signs of only partial water sublimation was the one shown in (Figure 3) and [1].

Results

Figure.1G shows a typical lower magnification picture of the Hong-Kong influenza virus. Round objects, as expected 50-100 nm diameter, are visible amid filaments and membranes (expected to be allantoic fluid [7]). Spherical virus is essentially of two types: with a hexagonal protrusion (Figure. 1A, B & D) or without it (Figure. 1C & E). Without a protrusion somewhat supporting the structures, virions appear flatter, or 'pancake' shape. But not always. In fact, the virion shown in Figure 2, demonstrated to be 3D by a tomogram, has not such hexagonal protrusion, and was seen partially shrank under illumination. Actually, also constructs of pure, unstained CA-HIV-1 [2] shrank under sustained illumination, contrary to [1].

It is well-known that the Hong-Kong influenza virus become tendentially round after many passages in chicken eggs (cfr. Figure. S1) [6]. Nevertheless, after TeC protocol virus appear quite different (Figures 1 and 2) from S1 and what is known for negative-stained influenza virus (see e.g. [7]). Corresponding results from a tomogram acquired on negative stained influenza virus in S2 demonstrate that after TeC the virus imaged was not collapsed. After virions were demonstrated to remain hemispherical when imaged after TeC (Figure 2), we observed that many virions deposited on the substrate show a hexagonal shape (protuberance) modifying their coat (Figure 1A. B, D). Actually, fluid-like material visually similar to part of some viral coats was found on the substrate next to all virions with a hexagonal shape in their top surface (Figures 1). It should also be noted that these TeC virus are opaque to this powerful accelerated electron beam. Probably because filled by stain, but possibly also because of the density of the organic material packed inside virions. Regardless the reason, such opacity to the radiation invalidates the usual optical assumption used for evaluating high-resolution TEM images (see e.g. [8]). Therefore, the seemingly 3D aspect of virions in Fig, 1 seems a real characteristic of in these images, distinguishing them from aggregates of colloidal gold without a virion found on the substrate. Actually, as proven as well by the presence of shadows in Figure. 1 A-E, similar to those casted by spherical objects under light. Finally, the hexagonal shape seen in many virions seems actually to correspond in size to the depressions found in air-dried stained virus (cfr. air-dried stained virions in S1, yellow arrow and [8]).

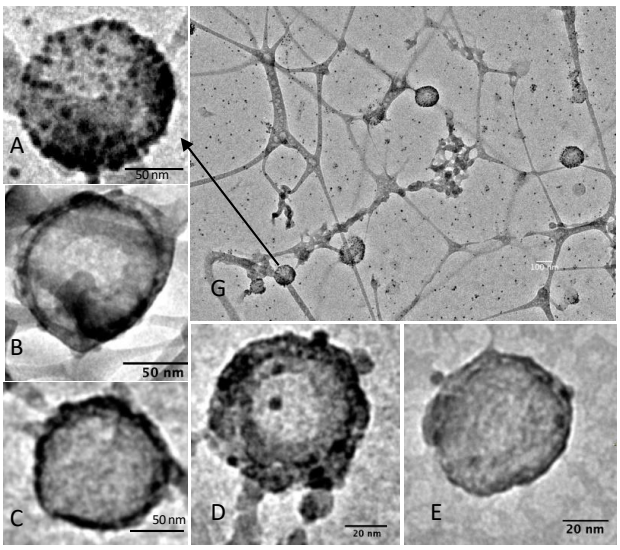

Figure 1: Influenza A virus of the Hong-Kong strain imaged at T≤–92ºC as described. G shows an overview at low magnification: many virions are recognizable, some with a somewhat flat, hexagonal top (arrow and A). The hexagonal motif is found in many virus (B and D) but not all (C and E). Virus deposited on the substrate are surrounded by a peculiar, seemingly liquid material which seems a preferential target of the colloidal gold particles (A-E). Interestingly, all virions seem impenetrable to radiation, as the shadow seen in A, C, E suggests, which observation is confirmed by the tomogram shown in Figure. 2.

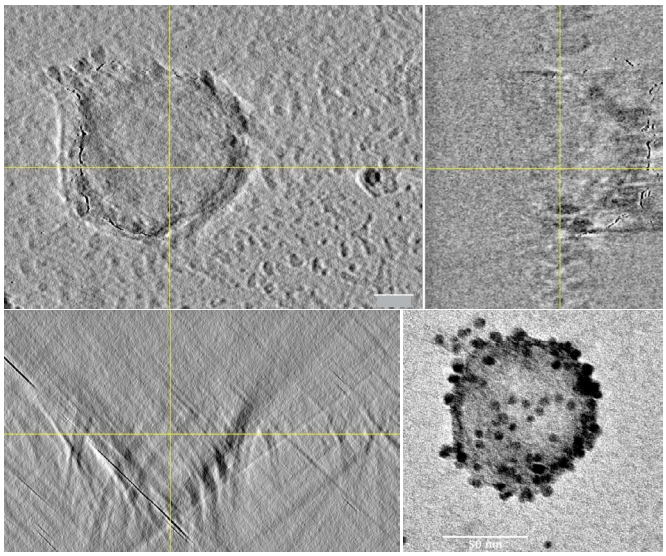

Figure 2: Influenza A Hong-Kong virus flash-frozen and stained, imaged after TeC. Spheres are 6 nm colloidal gold fiduciary markers. Top Left: XY plane from virtual section imaged at 0.1112 nm resolution; XZ plane on the right and YZ plane on the bottom. En-

face image pf the full virus before the tomography acquisition on the bottom right. In the XZ and YZ planes it is demonstrated that sample is three dimensional at the beginning of the experiment, although it shrank somewhat during the acquisition. Tomogram realized with images shot at 5,000 e–/nm2. This virus was remarkably thicker than the sample reported in S2. Scale bars: 20 or 50 nm.

Let us examine now images of microtubules assembled by pure (>99.6%) rat-brain tubulin (kind gift from the Unit for Cytoskeletal Dynamics, NICHD-NIH), which is a very hydrophobic protein that does not form convoluted membranes. In [1] it has been demonstrated that flash- frozen microtubules were undeformed by TeC when imaged frozen-solid at T~ –92ºC or lower. Well, in fact the workflow described in [1] allowed as well for the first time to take a peek into the world of microtubules in solution before solvent evaporated. Figure 3 shows a collection of images obtained from the same microtubules in [1]. Data in [1] correspond to microtubules deposited on the substate (shown in Figure 3A blue circle & B), imaged by tomography and shown to have the well-known diameter/characteristics, proving to be un-deformed by the workflow.

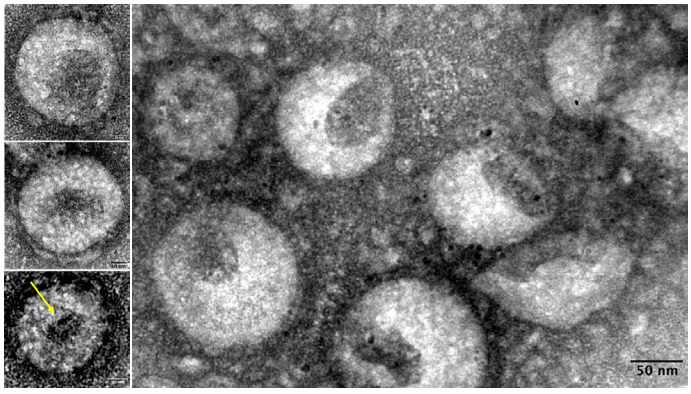

Figure 3: Microtubules assembled from rat brain tubulin as in [1] imaged at –92 ºC, flash-frozen after being (positive) stained with methyl-amine tungstate, as described. The 10 nm fiduciary markers were used in [1] for a tomogram in the area surrounded by a blue circle (Figure. 1A), corresponding to Figure 1B. In Figures. 1C and 1D microtubules are surprisingly shown also not completely straight, demonstrating in some cases a much lower bending rigidity that usually believed. Moreover, all these microtubules seem surrounded by a membrane, and some seem originating from the larger membrane (Figure. 1D) enclosing the microtubules. Only microtubules like Figure 1B have been imaged in [1].

But, when taken altogether, these images peculiarly show microtubules contiguous to a membrane (verisimilarly of 2D-tubulin). At lower magnifications, a membrane (Figure 3A) is seen extending over good part of the sample, and microtubules are seen strangely bent and contiguous to it (Figure 3A, C & D). In fact, microtubules in these conditions may seem to 'protrude' or be a 'constrained' portion of this 2D-tubulin membrane (Figures. 3C & D blue circle). Microtubules in these pictures are bent in a rather different way than what understandable within theoretical models accounting for their elasticity [9]. In the same experiment, straight, more rigid microtubules were also found on the surface of the supporting formvar-C film (Figures 3A, B). The blue circle in Fig. 3A shows the location of the microtubules in Figure 3B, corresponding to where the tomogram reported in [1] has been acquired, without suffering limitations from a high electron-dose (as demonstrated). Perhaps interestingly, the yellow arrow seems to indicate traces of what seem indications that microtubules changed position after initially 'falling' on the grid surface covered by stain. In fact, tomograms on traces like this showed not to contain any microtubule (data not shown).

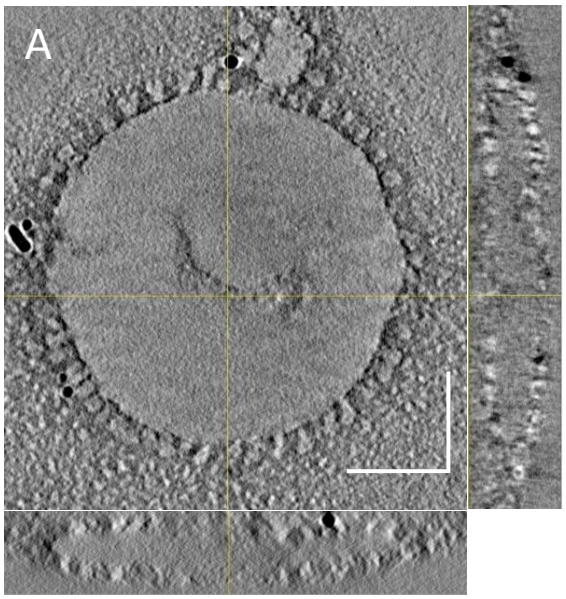

Figure S1: Negative stained Hong-Kong influenza A virions imaged after drying on the grid. The peculiar spherical shapes are always characterized by a darker area in the center of the virion, where the stain accumulates (as in [8]) maybe because of a depression of the structure caused by the evaporating water front.

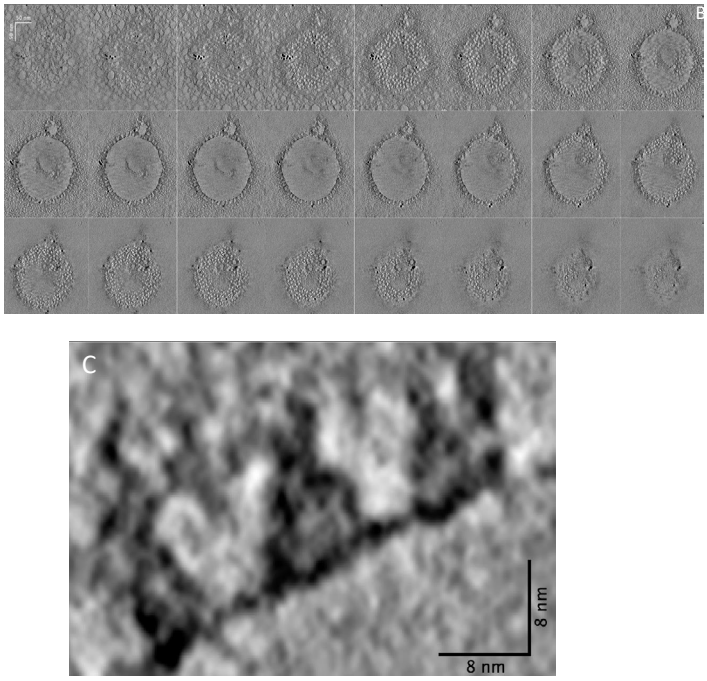

Figure S2: Virtual sections from a tomogram of air-dried influenza virus, negative stained with NanoW as in [8].
A: Perpendicular virtual sections from tomogram: in XZ and YZ plane virus appears less than
~20 nm thick.
B: virtual section ~1.4Å thick starting from the top left and through the whole thickness of the virion, where one section every 11 is plotted. It is evident that spikes are present at the top like at the bottom of the virion and it seems that some proteinaceous material is avulsed from the virus. C: Close-up XY virtual section of 2 spikes found on the surface of this virus.
White scale bars: 50 nm; Black Scale bars: 8 nm.

Discussion

When TeC results have been obtained for the first time [1], they were very puzzling since it was not clear how to eliminate possible artefacts. Just to name two possible causes: interaction of tubulin with the heavy-metal salt (tungstate) used may have created part of these images, as well as the rigidity of the biopolymers combined with the low-temperature curing protocol (TeC) used. Yet, the important fact emerging seemed that frozen biological structures temperature- preconditioned in this way could withstand the rigors intrinsic to a full tomography scan acquired with small defocus. Actually, these results do not contradict previous finding in [4] since those data were obtained with microtubules not protected by TeC from interactions with the radiation present in the sample [10, 11].

In order to approach these questions, TeC protocol has been demonstrated on assembled Capsid proteins extracted from the HIV-1 virus [2], which nevertheless are also not a very deformable substrate. Yet data in [2] demonstrate (1) the general applicability of TeC, and (2) the independence of electron-dose resistance from a metal salt used before flash-freezing, clarifying therefore that results do not depend on a heavy-metal ion coating (and fixing) the biologic structures [2]. Comparison of the data obtained with and without staining also seems to confine all modifications induced by heavy metal coating of these biological samples to distances smaller than one nanometer. Actually, the unexpected structures seen in [1] span hundreds of nanometers (until micrometers) length-scales. New experiments therefore were needed to further investigate such intriguing behavior. In this perspective here, we have presented direct images obtained on highly-deformable materials, i.e. influenza A Hong-Kong virus. Samples have been flash-frozen when deposited on an (inert) substrate, demonstrating that TeC is able to deliver undeformed biological samples able to sustain the rigors of a tomogram, independent on sample characteristics.

In some cases, partial shrinkage of samples has been observed after ~1 million e–/nm2. Such limitation seems to depend on the sublimation times used. Yet, the true question is: why samples were not all immediately vaporized by the radiation as in [4], which discussed flash- frozen but hydrated samples? Actually, if the shrinkage found in some samples will be managed, this method may become a possible approach to quickly view structures in cryo-immobilized biological samples, since valuable 3D data using this method can be obtained in a fraction of the time.

Probably, an explanation of this result could be hypothesized in light of modern descriptions of interactions between accelerated electrons and soft matter in an electron microscope [10], and maybe therefore interpreted in view of the quantization of energy necessary to realize energy exchanges. This quantization in fact implies the fact that there is interaction between photons and matter (including therefore ALL photons generated when accelerated particles target matter) only when there is availability of energy states of a suitable absorber chemical species. So, ONLY WHEN there is a suitable absorbing chemical species (atoms or molecules) where the energy is liberated there is absorption, otherwise photons (and molecules) radiate from the area unperturbed very quickly.

Such model actually seems appropriate to describe what happens in these samples [4]. In fact, if accelerated electrons incident on these samples could interact with the electronic energy levels available in the sample, let us enumerate possible absorbing candidates. Actually, the higher atomic electronic energy level available in this sample, which is the U 1s, is less than 80 keV. So, accelerated particles cannot be absorbed by the atomic energy levels of this sample. As it has been the case for the accelerated electron beam used in [1] and Fig. 3. Then, there is a gap of over 300 keV before arriving to lowest energetic levels of the nuclei (the first being above 400 keV).

Well, then what happened in [4]? Actually, when a beam of fast electrons penetrates a thin (solid) sample, it is well-known that bremsstrahlung radiation (E<2keV) is produced. Is there a chemical absorber for this radiation? Well, the most abundant chemical species in frozen hydrated samples are water molecules. And it is known that this radiation 'noise' corresponds to the region of absorption of the RAMAN spectroscopy [10, 11] of water molecules. Actually, there is the well-known water window, around 1.5 eV, where also OH groups absorb, but less strongly than the free-water molecules. In this interpretation, a plausible origin of some of the sample modifications consequent to electron beam irradiations would be melting of water molecules. In line with this proposed mechanism, the frozen samples shown here were resistant to sustained irradiation in a TEM after TeC because of sublimation of free-water molecules [5,6]. The remaining water molecules in the sample, bound to hydrophilic protein groups, would absorb at higher energy, which level is different enough for the molecule to be transparent to bremsstrahlung. Therefore, no melting should be observed in absence of ice in the sample, in line with these observations.

Further experiments, possibly substituting the solvent or maybe at higher resolution (using for instance aberration-corrected microscopes) are necessary to elucidate further such experimental results.

References

1. Fera, A. (2021). High-Resolution Electron Microscopy Tomography of Interacting Flash-Frozen Proteins. Systematic Reviews in Pharmacy, 13(1), 48-51.
2. Miao, J., Ercius, P., & Billinge, S. J. (2016). Atomic electron tomography: 3D structures without crystals. Science, 353(6306), aaf2157Chen, C. C., Zhu, C., White, E. R., Chiu, C. Y., Scott, M. C., Regan, B. C., ... & Miao, J. (2013). Three-dimensional imaging of dislocations in a nanoparticle at atomic resolution. Nature, 496(7443), 74-77.
3. Andrea Fera and Louis (Chip) Dye, Cryo-Fixed and Stained Microtubules Can Be Imaged With High Electron Doses Using The Full Resolving Power Of the Electron Microscope, doi:10.1017/S1431927617006237, Microsc. Microanal. 23 (Suppl 1), Pages. 1114-5, August 2017.
4. Leapman, R. D., & Sun, S. (1995). Cryo-electron energy loss spectroscopy: observations on vitrified hydrated specimens and radiation damage. Ultramicroscopy, 59(1-4), 71-79.
5. Wagner, W., Riethmann, T., Feistel, R., & Harvey, A. H. (2011). New equations for the sublimation pressure and melting pressure of H2O ice Ih. Journal of Physical and Chemical Reference Data, 40(4), 043103.
6. G. Jancso, J. Pupezin and W. A. Van Hook, The Vapor Pressure of Ice between + 10-2 and 10+20, The Journal of Physical Chemistry, Vol. 74, Vo. 15, 1970.
7. Hobley, D. E. J., Moore, J. M., & Howard, A. D. (2013, March). How rough is the surface of Europa at lander scale? In 44th Annual Lunar and Planetary Science Conference (No. 1719, p. 2432)
8. Zingsheim, H. P. (1984). Sublimation rates of ice in a cryo-ultramicrotome. Journal of microscopy, 133(3), 307-312.
9. Brauer, R., & Chen, P. (2015). Influenza virus propagation in embryonated chicken eggs. JoVE (Journal of Visualized Experiments), (97), e52421.
10. Fera, A., Farrington, J. E., Zimmerberg, J., & Reese, T. S. (2012). A negative stain for electron microscopic tomography. Microscopy and Microanalysis, 18(2), 331-335.
11. Lagomarsino, M. C., Tanase, C., Vos, J. W., Emons, A. M. C., Mulder, B. M., & Dogterom, M. (2007). Microtubule organization in three-dimensional confined geometries: evaluating the role of elasticity through a combined in vitro and modeling approach. Biophysical journal, 92(3), 1046-1057.
12. Tavernier, S. (2010). Experimental techniques in nuclear and particle physics (p. 306). Springer Nature.
13. Pastorczak, M., Kozanecki, M., & Ulanski, J. (2008). Raman resonance effect in liquid water. The Journal of Physical Chemistry A, 112(43), 10705-10707.